Available online at www.sciencedirect.com
ScienceDirect
Journal of Non-Crystalline Solids 354 (2008) 1948–1954
JOURNAL OF NON-CRYSTALLINE SOLIDS
www.elsevier.com/locate/jnoncrysol

Fabrication and properties of novel low-melting glasses in the ternary system $ZnO–Sb_2O_3–P_2O_5$

Bing Zhang [a], Qi Chen [a,b,*], Li Song [b], Huiping Li [b], Fengzhen Hou [b], Jinchao Zhang [b]

[a] Key Laboratory for Ultrafine Materials of Ministry of Education, East China University of Science and Technology, Shanghai 200237, China
[b] Department of Inorganic Materials, East China University of Science and Technology, Shanghai 200237, China

Received 19 July 2007; received in revised form 19 November 2007
Available online 30 January 2008

Abstract

Glasses in the ternary system $ZnO–Sb_2O_3–P_2O_5$ were investigated as potential alternatives to lead based glasses for low temperature applications. The glass-forming region of $ZnO–Sb_2O_3–P_2O_5$ system has been determined. Structure and properties of the glasses with the composition $(60 - x)ZnO–xSb_2O_3–40P_2O_5$ were characterized by infrared spectra (IR), differential thermal analysis (DTA) and X-ray diffraction (XRD). The results of IR indicated the role of Sb^{3+} as participant in glass network structure, which was supported by the monotonic and remarkable increase of density (ρ) and molar volume (V_M) with increasing Sb_2O_3 content. Glass transition temperature (T_g) and thermal stability decreased, and coefficient of thermal expansion (α) increased with the substitution of Sb_2O_3 for ZnO in the range of 0–50 mol%. XRD pattern of the heat treated glass containing 30 mol% Sb_2O_3 indicated that the structure of antimony–phosphate becomes dominant. The improved water durability of these glasses is consistent with the replacement of easily hydrated phosphate chains by corrosion resistant P–O–Sb bonds. The glasses containing $\geqslant 30$ mol% Sb_2O_3 possess lower T_g (<400 °C) and better water durability, which could be alternatives to lead based glasses for practical applications with further composition improvement.

PACS: 61.10.Nz; 65.60.+a; 68.37.−d

Keywords: Chemical durability; X-ray diffraction; Phosphates; Glass transition

1. Introduction

Lead based low-melting glasses have been employed for most commercial applications, such as adhesives for glass, ceramic or metal materials, sealing or coating frits for electronic components, conductive or resistive pastes [1–3]. Unfortunately, lead based glasses contain a great quantity of PbO, which is deleterious to health and environment [4,5]. New lead free low-melting glasses are being studied during recent years. The unique physical properties, including high coefficient of thermal expansion (α), low glass transition temperature (T_g), of phosphate glasses make them superior to silicate and borosilicate glasses for low-melting application as alternatives to lead based glasses [6–8]. However, problem that has been highlighted of such systems is that they usually have poor water durability due to the existence of easily hydrated phosphate chains. Recent results indicate that it is possible to prepare phosphate glasses with excellent resistance to aqueous corrosion by adding such metal oxides with high valence cations like Fe_2O_3, Al_2O_3, etc., to phosphate glasses [9,10], but resulting in an increase in T_g significantly.

The improvement of water durability of phosphate glasses containing SnO has also been proved [11], and $ZnO–P_2O_5$ glasses containing large amount of SnO have attracted extensive investigation in recent years [12–14]. These glasses posses lower T_g and excellent water durability that make them suitable for potential alternative to lead

* Corresponding author. Address: Department of Inorganic Materials, East China University of Science and Technology, 130 Meilong Road, Xuhui District, Shanghai 200237, China. Tel.: +86 21 64253466; fax: +86 21 64250882.
E-mail address: qichen@ecust.edu.cn (Q. Chen).

0022-3093/$ - see front matter © 2007 Elsevier B.V. All rights reserved.
doi:10.1016/j.jnoncrysol.2007.11.007

glasses. But the fluctuation problem of T_g of tin-containing zinc phosphate glasses, due to the oxidation of tin from +2 valance to +4 valance, could not be eliminated completely, thereby rendering it undesirable for industrial application [15]. Moreover, from a cost standpoint, the extensive use of SnO will lead to a remarkably increase in cost of glass raw materials. As such there remains a need for tin-free low-melting glasses for practical application.

Theoretically, glasses containing Sb_2O_3 will also have low melting and transition temperatures as Sb^{3+} has a lone electron pair [16]. And Sb_2O_3 is much cheaper than SnO. Ghost and Chaudhuri [17] synthesized Sb_2O_3-containing V_2O_5–P_2O_5 glasses with lower T_g and improved stability against moisture under ambient conditions. Koudelka et al. [18] found that the incorporation of Sb_2O_3 into borophosphate network of $50ZnO–10B_2O_3–40P_2O_5$ glasses modified its structure and decreased the T_g values. However, there has been no experiment conducted to evaluate the structure and properties of ternary glasses in the system $ZnO–Sb_2O_3–P_2O_5$. With a view to develop new low-melting glasses, the ternary $ZnO–Sb_2O_3–P_2O_5$ glasses were prepared and characterized in this study.

2. Experimental procedure

2.1. Glass preparation

The raw materials used in the preparation of $ZnO–Sb_2O_3–P_2O_5$ glasses were reagent grade zinc phosphate ($Zn_3(PO_4)_2 \cdot 4H_2O$), antimony trioxide (Sb_2O_3), and phosphorus pentoxide (P_2O_5). The 100 g batch was thoroughly mixed and pre-treated at 260 °C for 4 h to avoid the volatility of P_2O_5 at high temperature, and then melted using a high-purity alumina crucible at 930–1050 °C for 1 h. Melting conditions were optimized to produce a minimal Al_2O_3 pickup from the crucible and a minimal volatility of Sb_2O_3. Each melt was stirred two times in a step of 20 min. The homogenous melt was cast into a preheated steel plate to form a rectangular block. The block was properly annealed at 10 °C above the T_g for 2 h, and then slowly cooled to room temperature in a muffle furnace. The glass samples were kept in a desiccator before using.

2.2. Methods of analysis

Infrared spectra of the glass samples were measured on an infrared spectrophotometer (TJ270-30A, TJ Photics, China) using KBr pellet method. Differential thermal analyzer (SDT Q600, TA instruments, USA) was used to detect the glass transition temperature (T_g) and thermal stability of the glass samples under a heating rate of 10 °C/min. An approximate measure of the thermal stability of each glass is determined from the temperature difference, ΔT, between the first crystallization temperature and T_g. X-ray diffraction patterns of the glass samples after heating were collected using an X-ray diffractometer (D/MAX-rB, Rigaku, Japan). Coefficients of thermal expansion (α, 50–300 °C) were measured by a horizontal dilatometer at a heating rate of 4 °C/min. Glass density (ρ) of the bulk samples was measured at room temperature by the Archimedes' method using ethanol as the suspending medium. The molar volume (V_M) was calculated using the expression $V_M = M/\rho$, where M is the average molar weight of the glass. The errors in T_g, α, and ρ are estimated at ±2 °C, $\pm 2 \times 10^{-7}$ °C^{-1} and ±0.02 g/cm^3, respectively.

Water durability of the bulk glasses were evaluated from their weight loss of per unit surface area in deionized water (pH ≈ 6.70) at 50 °C for 1 day, and at 90 °C for up to 5 days. Rectangular samples (approximately $30 \times 20 \times 5$ mm^3) were cut, ground, polished, cleaned and weighted (±0.1 mg). The dimensions were measured before suspending the glass samples in a thermostatic tank containing 4 L deionized water, which was heated and hold at 50 or 90 °C. Each sample was removed from the thermostatic tank after immersion for per day, dried in an oven at 120 °C for 2 h and weighted. After the samples have been removed, the deionized water in the thermostatic tank was replaced by fresh water. Duplicate measurements were made. Microscopic appearance of the samples before and after immersion in deionized water at 90 °C for 5 days was observed by a binocular microscope (Leitz Ortholux II POL-BK, Germany). The loss of deionized water for each cycle is estimated at 5%, and the error in weight loss is estimated at ±10%.

3. Results

The approximate region for glass formation in the ternary system $ZnO–Sb_2O_3–P_2O_5$ is illustrated in Fig. 1. Open and close circles denote transparent and crystallized samples confirmed by XRD respectively, while half-open circles denote opaque samples without crystallization. It was observed that the glass-forming region crosses the entire ternary system, from 40 to 70 mol% P_2O_5. The glass samples with high content of Sb_2O_3 ($\geqslant$20 mol%) were typically yellow in color, which became more noticeable with increasing Sb_2O_3 content. The surface of samples with P_2O_5 content $\geqslant$50 mol% became white after several weeks

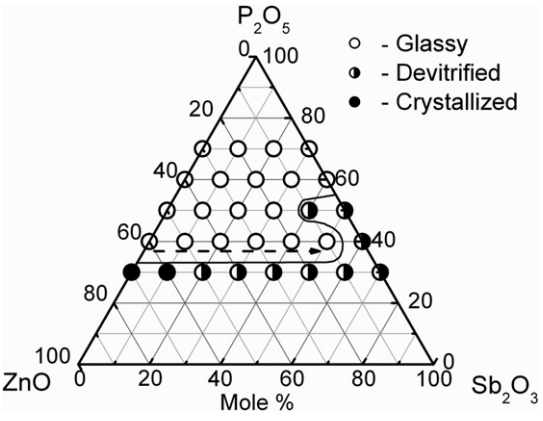

Fig. 1. Glass formation region of the ternary system $ZnO–Sb_2O_3–P_2O_5$.

in air, very likely due to reaction with humidity. It is suggested that the glasses containing high amount of P_2O_5 are hygroscopic, and not suitable for practicable applications. Thus P_2O_5 content of the glass samples chosen for present study was fixed on 40 mol% (see Table 1), as drawn in Fig. 1 by dash line. Effect of the replacement of ZnO by Sb_2O_3 on the glass structure and properties was investigated.

3.1. IR spectra, DTA and XRD measurements

Infrared spectra of the glass samples are shown in Fig. 2. For the spectrum of Sb0 glass, the $\nu_{as}(PO_2)$ and $\nu_s(PO_2)$ vibrations of the O–P–O bonds of Q^1 and Q^2 tetrahedra with non-bridging oxygens (O_{NB}) are observed around 1263 and 1090 cm^{-1} respectively, whereas the absorption peaks around 926 and 739 cm^{-1} are ascribed to the asymmetric and symmetric vibrations of P–O–P bonds of bridging oxygens (O_B) in phosphate chains [19–22]. The strong band around 505 cm^{-1} is the absorption peak of bending vibration of P–O bonds, δ(P–O), of Q^0 tetrahedra with non-bridging oxygens. The phosphate tetrahedra are classified using the Q^i terminology, where 'i' represents the number of bridging oxygens per tetrahedron [22]. A new absorption peak around 628 cm^{-1}, assigned following Sudarsan and Kulshreshtha [23] to the stretching vibration of P–O–Sb linkages, appears in the infrared spectra of these Sb_2O_3-containing glasses. With an increase of Sb_2O_3 content as shown in Fig. 2, these absorption peaks in the high frequency range become broader, less distinct and overlap each other.

Fig. 3 shows the DTA curves of the synthesized glasses. Characteristic temperatures of the glasses (T_g for glass transition temperature, T_{c1} and T_{c2} for crystallization temperatures) are summarized in Table 2. It is found that T_g shifts monotonously to lower temperature with increasing Sb_2O_3 content from 422 °C for Sb0 glass to 377 °C for Sb50 glass, and the crystallization temperature T_{c1} decreases firstly and then increases with a reduction in its amplitude. A new crystallization peaks, T_{c2}, presents in the DTA curves and shifts to a lower temperature for the glass sample containing $\geqslant$30 mol% Sb_2O_3. Following the ΔT value of the samples, one observes a higher value for Sb10 glass, which means a more stable glass forming ability. The ΔT value decreases by further addition of Sb_2O_3.

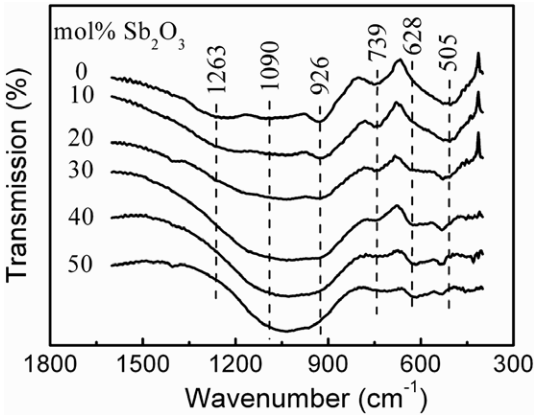

Fig. 2. Infrared spectra of the $(60 - x)ZnO–xSb_2O_3–40P_2O_5$ glasses.

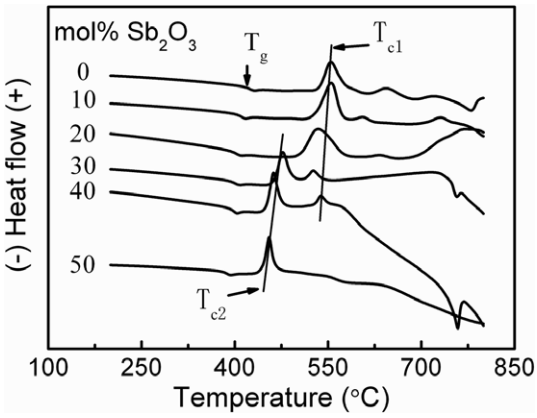

Fig. 3. DTA curves of the $(60 - x)ZnO–xSb_2O_3–40P_2O_5$ glasses under a heating rate of 10 °C/min.

Table 2
Thermal properties for $(60 - x)ZnO–xSb_2O_3–40P_2O_5$ glasses from DTA

Sample	T_g (±2 °C)	T_{c1} (±2 °C)	T_{c2} (±2 °C)	ΔT (°C)
Sb0	422	554	No peak	132
Sb10	407	555	No peak	148
Sb20	402	534	No peak	132
Sb30	393	526	476	83
Sb40	384	540	463	79
Sb50	377	No peak	455	78

ΔT is the temperature difference between the first crystallization temperature and T_g.

Table 1
Batch composition of the glasses in $(60 - x)ZnO–xSb_2O_3–40P_2O_5$ system (mol%)

Sample	P_2O_5	Sb_2O_3	ZnO	Melting temperature (°C)	Color	O/P molar ratio	α (±2 × 10^{-7} $°C^{-1}$)
Sb0*	40	0	60	1050	Colorless	3.25	74
Sb10	40	10	50	1000	Colorless	3.50	80
Sb20	40	20	40	980	Pale yellow	3.75	98
Sb30	40	30	30	960	Pale yellow	4.00	108
Sb40	40	40	20	950	Yellow	4.25	115
Sb50	40	50	10	930	Yellow	4.50	122

* Sb denotes the $ZnO–Sb_2O_3–P_2O_5$ glass given in the table, and the next number denotes the molar percent of Sb_2O_3 in the glass.

Small portions of the glasses containing 0, 20, and 30 mol% Sb_2O_3 were crystallized by heating for 4 h in air at 564, 544, and 486 °C, respectively which correspond to the temperatures of the first crystallization peak in the DTA curves (see Fig. 3). The resulting XRD patterns shown in Fig. 4 indicate that the major crystalline phase changes with the substitution of different amount Sb_2O_3: $Zn_2P_2O_7$ (PDF#34-1275) for Sb0 glass and $SbPO_4$ (PDF#35-0829) for Sb30 glass, and the crystalline phase that existed in the $40ZnO–20Sb_2O_3–40P_2O_5$ glass was not identified by the PDF cards. An unknown Zn–Sb–P–O compound might be formed after heating for the glass.

3.2. Density and molar volume

The density (ρ) and molar volume (V_M) of the glasses are shown in Fig. 5. It can be seen that ρ increases linearly from 3.34 to 4.17 g/cm^3 with increasing Sb_2O_3 content. Obviously, the increase is mainly due to the much higher mass molar weight of Sb_2O_3 than that of ZnO [24]. There is also a linear increase in V_M (from 31.9 cm^3/mol for $x = 0$ to 50.5 cm^3/mol for $x = 50$) of $(60 - x)ZnO–xSb_2O_3–40P_2O_5$ glasses in the same region.

3.3. Water durability

For the phosphate glasses containing different amount of Sb_2O_3, the water durability as determined by the sample weight loss in deionized water at 50 °C for 1 day is shown in Fig. 6. The water durability of these glasses is found to be sensitive to the glass composition. It can be seen clearly that the glasses whose Sb_2O_3 content is $\geqslant 10$ mol% have much better water durability (less weight loss), which increases with increasing amount of Sb_2O_3. Weight loss decreases from 26.1 mg/cm^2 for Sb0 glass to 1.3 mg/cm^2 for Sb50 glass.

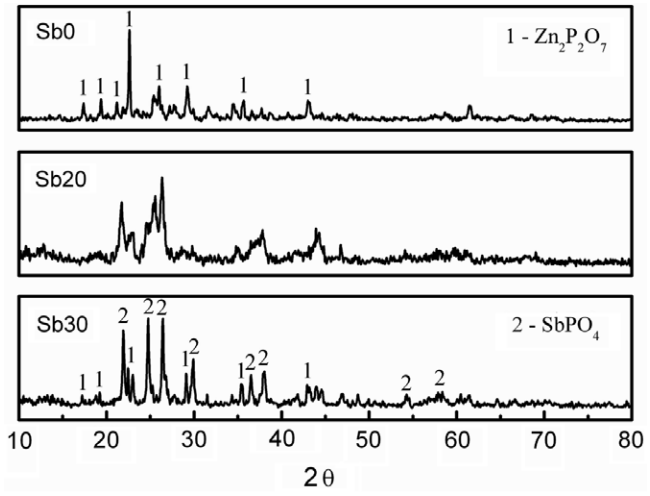

Fig. 4. X-ray diffraction patterns of Sb0, Sb20, and Sb30 glasses after heating. '1' and '2' denote the crystalline phase of $Zn_2P_2O_7$ (PDF#34-1275) and $SbPO_4$ (PDF#35-0829), respectively identified by the PDF card.

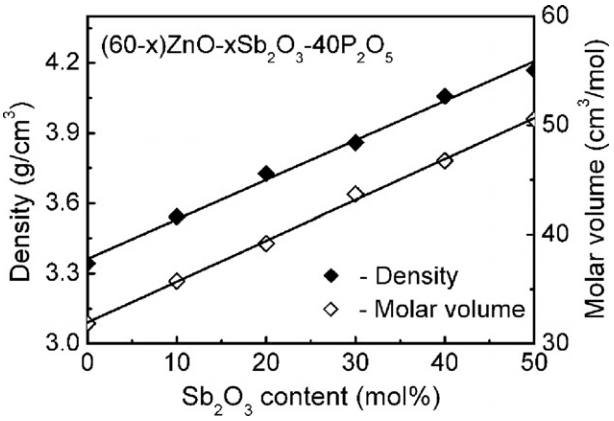

Fig. 5. Density (ρ) and molar volume (V_M) as functions of Sb_2O_3 content of the $(60 - x)ZnO–xSb_2O_3–40P_2O_5$ glasses. The error of ρ is estimated at ±0.02 g/cm^3.

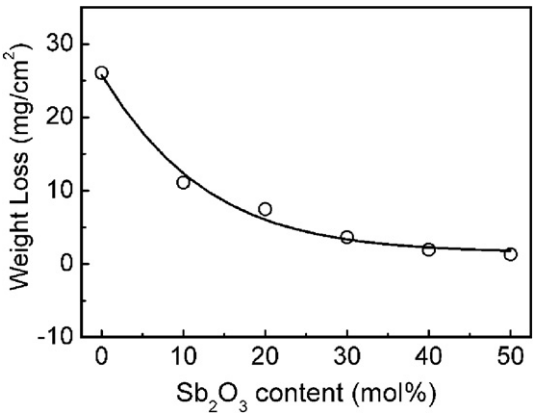

Fig. 6. Water durability of $(60 - x)ZnO–xSb_2O_3–40P_2O_5$ glasses as a function of Sb_2O_3 content after immersion in deionized water at 50 °C for 1 day. The error of weight loss is estimated at ±10%.

The glasses containing 30, 40, and 50 mol% Sb_2O_3, which have better water durability in 50 °C water, were also evaluated for water durability in deionized water at 90 °C for up to 5 days (see Fig. 7). Obviously, weight loss of each glass after immersion in 90 °C water is much higher than that in 50 °C. The average weight loss of Sb50 glass, for example, is 6.7 mg/cm^2/day after immersion for 5 days. The curves of weight loss verse immersion time (days) are approximate straight lines, which means an approximate stable dissolution in water of these glasses. It was also observed that the pH values of the solutions in which the glass samples were immersed at 50 and 90 °C decreased from neutral (≈6.7) to acid.

In order to show more clearly where the optimum glass may lie, T_g and thermal stability ΔT plotted against the water durability of the glasses are illustrated in Fig. 8. The water durability is determined by the weight loss in water at 50 °C for 1 day (see Fig. 6). It can be seen that T_g decrease with increasing durability, indicating that the substitution of Sb_2O_3 for ZnO is beneficial to develop the glass composition with both improved durability and lower

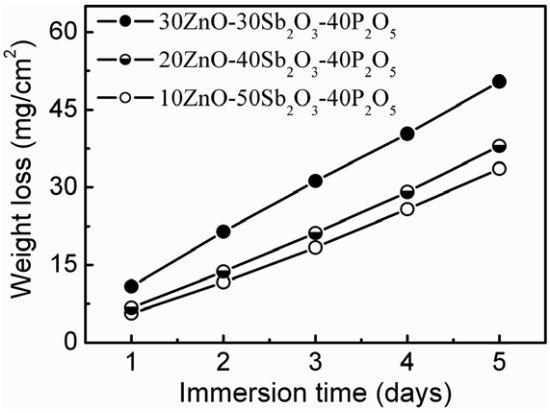

Fig. 7. Water durability of the glasses containing 30, 40 and 50 mol% Sb_2O_3 as a function of immersion time in deionized water at 90 °C for up to 5 days. The error of weight loss is estimated at ±10%.

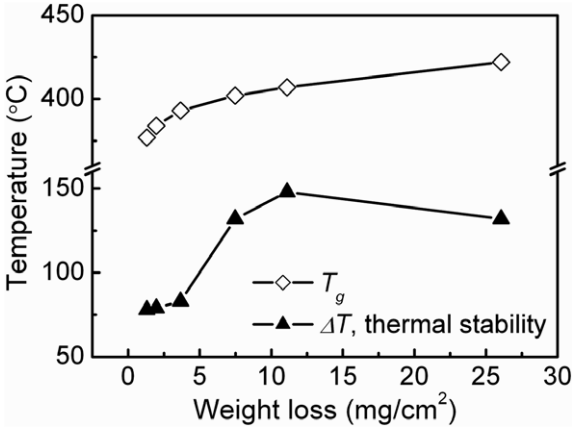

Fig. 8. Glass transition temperature T_g and thermal stability ΔT plotted as functions of the water durability of $(60 - x)$ZnO–$x$$Sb_2O_3$–40$P_2O_5$ glasses. The water durability is determined by the weight loss after immersion in water at 50 °C for 1 day.

T_g. The variation of ΔT, except for that of Sb10 glass, as the function of the durability exhibits the same characteristic as T_g.

4. Discussion

The IR results indicate that Sb_2O_3 participates in the glass network, as the intensity of the new band around 628 cm^{-1} (see Fig. 2), ascribed to the stretching vibration of P–O–Sb linkages, increases with increasing amount of Sb_2O_3. The remarkable increase of molar volume (V_M) (see Fig. 5) supports this deduction. No change in the slopes of ρ and V_M with composition suggests no change in structural role of Sb_2O_3 in these glass samples [25]. Although as glass network participant, the substitution of Sb_2O_3 for ZnO does not expand the glass-forming region remarkably. As mentioned hereinafter, the local structure of Sb^{3+} is less symmetric and the field strength of Sb^{3+} is much higher than that of Zn^{2+}, which will cause the glass containing large amount of Sb_2O_3 devitrified or even crystallized.

The IR band around 505 cm^{-1}, which is due to the bending vibration of P–O bonds of Q^0 tetrahedra, decreases in intensity with increasing Sb_2O_3 content, while the $\nu_{as}(PO_2)$ vibration around 1263 cm^{-1} disappears. This indicates that P–O–Sb linkages are formed from the polymerization of $P–O_{NB}$ bonds with Sb^{3+} cations. The shift towards high frequency of δ(P–O) mode may well arise from the higher field strength of Sb^{3+} cation [24]. Sudarsan and Kulshreshtha [23] observed that there are three P–O stretching vibrations of P–O–Sb linkages at ∼ 1140, 1060, and 962 cm^{-1} respectively. Thus it can be deduced reasonably that the overlapping of these absorption peaks and the peaks derived from phosphate network (∼1263, 1090, and 926 cm^{-1}) should, at least partly, respond for the broadening in the high frequency range.

Even though the structure of a glass may not be identical to its crystalline counterpart, it is reasonable to expect to general similarities between the crystal and glass structure [26]. The XRD results of the ternary samples reveal the change of glass structure with the substitution of Sb_2O_3, and for the glass containing 30 mol% Sb_2O_3 the structure of antimony–phosphate becomes dominant. The general structure of the glasses containing 30 mol% Sb_2O_3 can be visualized as consisting of PO_4 tetrahedra and SbO_3 pyramids [27] joined together by bridging oxygens.

Sb^{3+} has a lone electron pair, which occupies a greater angular volume than a bonding pair of electrons. As a participant of glass network, the local structure of Sb^{3+} cations become less symmetric and the strain energy in the glass network increases as a whole, thus resulting in a decrease in the additional activation energy which is necessary for glass network rearrangement [16]. So that there will be an almost linear increase in α (see Table 1) and decrease in T_g (see Table 2) of the glasses with increasing amount of Sb_2O_3.

The electrostatic field around SbO_3 pyramids with −3 charge presented in the glass attracts Zn^{2+} cations, which will increase the activation energy for crystallization of Zn^{2+} and PO_4 units. Thus there is an increase in glass thermal stability when 10 mol% ZnO was substituted by Sb_2O_3. But on the other hand, as mentioned hereinbefore, the further addition of Sb_2O_3 will cause the rearrangement of glass network easier, namely will decrease the glass thermal stability. A new crystallization peak T_{c2} in the DTA curves of the glass containing $\geqslant$30 mol% Sb_2O_3 was attributed to the formation of $SbPO_4$ as proved from the XRD patterns shown in Fig. 4. The formation of $SbPO_4$ at lower temperature decreases the crystallization degree of zinc–phosphate crystal. So the crystallization peak, T_{c1}, decreases in intensity and shifts to higher temperature, even disappears in the DTA curve of the glass containing 50 mol% Sb_2O_3.

It is well known that the poor water durability of phosphate glasses is due to the breaking and dissolution of phosphate chains into water [9,28]. The change of solution pH from neutral to acid supports the dissolution process in

the present study. As participant of glass network, Sb^{3+} provides a stronger crosslink between phosphate tetrahedra. The interlinkage of highly dissolvable P–O_{NB} by Sb^{3+} and the replacement of easily hydrated phosphate chains by corrosion resistant P–O–Sb bonds improve the durability of the glass samples undoubtedly. Thus the glass containing larger amount of Sb_2O_3 have better water durability (less weight loss).

One may suspect that why the P–O–Sb bonds are corrosion resistant. Sb^{3+} has a higher polarizing power ($\approx$ valence/radius, valence = +3, radius = 0.89 Å) [25], which causes the oxygen attached to it to have a lower basicity or, in other word, a lower concentration of negative charge. It therefore serves to reduce its attraction to the positive ends, namely H^+ ions, of H_2O molecules [11]. On the other hand, the lone pair of electrons of Sb^{3+} located at the top of SbO_3 pyramid [27,29] strongly attracts the positive ends of H_2O molecules, which will decrease the attack of H^+ ions to P–O bonds of P–O–Sb linkages. The resulting increase of water durability of phosphate glasses with the addition of Sb_2O_3 can be described by the following reaction mechanism visually:

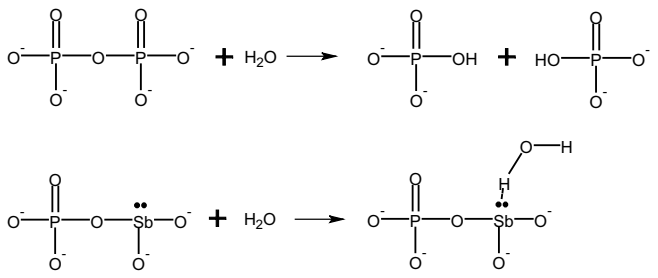

The relationship of water durability and O/P molar ratio of these glass samples is also considered. As can be seen in Table 1 and Fig. 6, the optimum O/P ratio (best water durability) for the present work is 4.50. According to the previous theoretical analyses on the mechanism and kinetics of dissolution for phosphate glasses, however, the optimum ratio would more reasonably close to 3.50 [26], which corresponds to the structure Q^1 where two PO_4 tetrahedra join together to form pyrophosphate (P_2O_7) groups. The disagreement may be shed light on the fact that Sb_2O_3 participate in glass network in the present study and seize a portion of oxygen ions to form SbO_3 pyramids, resulting in a change of the glass network structure. The water durability of PO_4–SbO_3 groups is better than that of PO_4–PO_4, namely P_2O_7, groups.

Although the addition of $\geqslant$30 mol% Sb_2O_3 to 60ZnO–$40P_2O_5$ glass decreases the thermal stability remarkably (see Table 2 and Fig. 8), these glasses are still deemed to be the optimum as they possess both lower T_g and better water durability. And our further work has indicated that thermal stability, rather than T_g or durability, of the glasses could be improved relatively easier with composition improvement.

As mentioned above, in comparison with ZnO–P_2O_5 binary glasses, low-melting glasses based on the ZnO–Sb_2O_3–P_2O_5 ternary system containing $\geqslant$30 mol% Sb_2O_3 possess the advantageous physical properties of lower T_g (<400 °C) and better water durability. It can be considered reasonably that, with further adjustment of glass composition, such system is a possible alternative to lead based glasses used as sealing frits for plasma display apparatus and transparent dielectric layer for plasma display panel, etc.

5. Conclusions

The glass-forming region of ZnO–Sb_2O_3–P_2O_5 ternary glasses has been determined, and structure and properties of the glasses with the composition $(60 - x)$ZnO–xSb_2O_3–$40P_2O_5$ (x = 0–50 mol%) have been investigated. Sb^{3+} cations participate in the glass network and polymerize with P–O_{NB} bonds to form P–O–Sb linkages. The substitution of Sb_2O_3 for ZnO results in:

- an increase in density, molar volume and coefficient of thermal expansion;
- a decrease in glass transition temperature and thermal stability;
- an improved water durability, which is attributed to the easily hydrated phosphate chains being replaced by corrosion resistant P–O–Sb bonds.

The glasses containing $\geqslant$30 mol% Sb_2O_3 possess lower T_g (<400 °C) and better water durability, which could be alternative to lead based glasses for practical applications with further composition improvement.

References

[1] S. Hasegawa, M. Kanai, T. Kamimoto, H. Torii, US Patent 2004012883, 2004.
[2] S. Kenneth, T. Christopher, D. Timothy, W. Christopher, US Patent 2004018930, 2004.
[3] S. Fujino, C. Hwang, K. Morinaga, J. Am. Ceram. Soc. 87 (1) (2004) 10.
[4] RoHS (The Restriction of the Use of Certain Hazardous Substances in Electrical and Electronic Equipment), a directive adopted in February 2003 by the European Union.
[5] S. Ogihara, New Glass 13 (3) (1998) 32.
[6] G.H. Beall, C.J. Quinn, US Patent 4940677, 1990.
[7] R.K. Brow, D.R. Tallant, J. Non-Cryst. Solids 222 (1997) 396.
[8] Y. Dotani, H. Usui, T. Manabe, JP Patent 2001180972, 2001.
[9] X. Yu, D.E. Day, G.J. Long, R.K. Brow, J. Non-Cryst. Solids 215 (1997) 21.
[10] R.K. Brow, L. Kovacic, US Patent 5262364, 1993.
[11] A.E. Marino, S.R. Arrasmith, L.L. Gregg, S.D. Jacobs, G.R. Chen, Y.J. Duc, J. Non-Cryst. Solids 289 (2001) 37.
[12] G.L. Fransic, R. Morena, US Patent 5281560, 1994.
[13] R. Morena, J. Non-Cryst. Solids 263&264 (2000) 382.
[14] K. Taketami, JP Patent 2003252648, 2003.
[15] C.J. Quinn, WO Patent 02057195, 2002.
[16] H. Niida, M. Takahashi, T. Uchino, T. Yoko, J. Non-Cryst. Solids 306 (2002) 292.
[17] A. Ghost, B.K. Chaudhuri, J. Non-Cryst. Solids 103 (1988) 83.

[18] L. Koudelka, J. Šubčík, P. Mošner, L. Montagne, L. Delevoye, J. Non-Cryst. Solids 353 (2007) 1828.
[19] K. Mayer, J. Non-Cryst. Solids 209 (1997) 227.
[20] A.M. Efimov, J. Non-Cryst. Solids 209 (1997) 209.
[21] L. Koudelka, P. Mošner, Mater. Lett. 42 (2000) 194.
[22] R.K. Brow, J. Non-Cryst. Solids 263&264 (2000) 1.
[23] V. Sudarsan, S.K. Kulshreshtha, J. Non-Cryst. Solids 286 (2001) 99.
[24] B.H. Jung, D.N. Kim, H.S. Kim, J. Non-Cryst. Solids 351 (2005) 3356.
[25] M.M. Karim, D. Holland, Phys. Chem. Glasses 36 (1995) 206.
[26] G.K. Marasinghe, M. Karabulut, C.S. Ray, D.E. Day, C.H. Booth, P.G. Allen, D.K. Shuh, Ceram. Trans. 87 (1998) 261.
[27] A. Datta, A.K. Giri, D. Chakravorty, Phys. Rev. B 47 (1993) 16242.
[28] H. Takebe, Y. Baba, M. Kuwabara, J. Non-Cryst. Solids 352 (2006) 3088.
[29] J.M. Philip, A.C. Charles, Spectrochim. Acta 38A (5) (1982) 555.